Radiology

Left Ventricular Long-Axis Function Assessed with Cardiac Cine MR Imaging Is an Independent Predictor of All-Cause Mortality in Patients with Reduced Ejection Fraction: A Multicenter Study[1]

Simone Romano, MD
Robert M. Judd, PhD
Raymond J. Kim, MD
Han W. Kim, MD
Igor Klem, MD
John F. Heitner, MD
Dipan J. Shah, MD
Jennifer Jue, MD
Afshin Farzaneh-Far, MD, PhD

Purpose: To evaluate the prognostic value of a simple index of left ventricular (LV) long-axis function—lateral mitral annular plane systolic excursion (MAPSE)—in a large multicenter population of patients with reduced ejection fraction (EF) who were undergoing cardiac magnetic resonance (MR) imaging.

Materials and Methods: This retrospective study included 1040 consecutive patients (mean age, 59.5 years ± 15.8) at four U.S. medical centers who were undergoing cardiac MR imaging for assessment of LV dysfunction with EF less than 50%. Lateral MAPSE was measured in the four-chamber cine view. The primary end point was all-cause death. Cox proportional hazards regression modeling was used to examine the independent association between lateral MAPSE and death. The incremental prognostic value of lateral MAPSE was assessed in nested models.

Results: During a median follow-up of 4.4 years, 132 patients died. With Kaplan-Meier analysis, the risk of death increased significantly with decreasing tertiles of lateral MAPSE (log-rank $P = .0001$). Patients with relatively preserved lateral MAPSE (>9 mm) had very few deaths, regardless of whether their EF was above or below 35%. Patients with late gadolinium enhancement (LGE) and low lateral MAPSE had significantly reduced survival compared to those with LGE and high lateral MAPSE (log-rank $P < .0001$). Lateral MAPSE was independently associated with risk of death after adjustment for clinical and imaging risk factors, which were univariate predictors (age, body mass index, diabetes, LV end-diastolic volume index, LGE, EF) (hazard ratio = 2.051 per mm decrease; 95% confidence interval [CI]: 1.520, 2.768; $P < .001$). Inclusion of lateral MAPSE in this model resulted in significant improvement in model fit (likelihood ratio test $P < .0001$) and C statistic (increasing from 0.675 to 0.844; $P < .0001$). Continuous net reclassification improvement was 1.036 (95% CI: 0.878, 1.194).

Conclusion: Lateral MAPSE measured during routine cine cardiac MR imaging is a significant independent predictor of mortality in patients with LV dysfunction, incremental to common clinical and cardiac MR risk factors—including EF and LGE.

[1] From the Division of Cardiology, Department of Medicine, University of Illinois at Chicago, 840 S Wood St, M/C 715, Suite 920 S, Chicago, IL 60612 (S.R., J.J., A.F.F.); Department of Medicine, University of Verona, Verona, Italy (S.R.); Division of Cardiology, Department of Medicine, Duke University, Durham, NC (R.M.J., R.J.K., H.W.K., I.K., A.F.F.); Department of Cardiology, New York Methodist Hospital, Brooklyn, NY (J.F.H.); and Houston Methodist DeBakey Heart & Vascular Center, Houston, Tex (D.J.S.).
Received March 6, 2017; revision requested April 17; revision received June 16; accepted June 20; final version accepted June 27. **Address correspondence to** A.F.F. (e-mail: *afshin@uic.edu*).

R.M.J. was supported in part by National Institutes of Health grant R42-HL117397, and R.J.K. was supported in part by National Institutes of Health grant R01-HL64726.

Long-axis atrioventricular plane displacement appears to play a fundamental role in cardiac mechanics and has been shown to be an important contributor to left ventricular (LV) pumping in both health and disease (1,2). Moreover, long-axis dysfunction appears to be an early marker for a number of pathologic states (3).

Assessment of long-axis function by using echocardiography has been shown to provide independent prognostic information in a wide variety of cardiac conditions, including LV dysfunction (4,5). Recently, the prognostic value of lateral mitral annular plane systolic excursion (MAPSE) as an index of long-axis function was suggested in a single-center cardiac magnetic resonance (MR) imaging study of unselected patients with preserved and reduced ejection fraction (EF) (6). We therefore hypothesized that lateral MAPSE measured during cine cardiac MR imaging may provide independent prognostic information in patients with LV dysfunction.

The aim of this study was to evaluate the prognostic value of a simple index of LV long-axis function, lateral MAPSE, in a large multicenter population of patients with reduced EF undergoing cardiac MR imaging.

Advances in Knowledge

- Lateral mitral annular plane systolic excursion (MAPSE), as a surrogate for left ventricular (LV) long-axis function, can be measured with low inter- and intraobserver variability from conventional cine cardiac MR images.
- At Kaplan-Meier analysis, the risk of death increases significantly with decreasing tertiles of lateral MAPSE (log-rank P = .0001).
- Lateral MAPSE is a significant independent predictor of all-cause death in patients with reduced ejection fraction (EF) after adjustment for clinical and imaging risk factors (hazard ratio = 2.051 per mm decrease; 95% confidence interval [CI]: 1.520, 2.768; $P < .001$); in other words, every 1-mm decrease in lateral MAPSE is associated with an approximately twofold increase in death.
- The addition of lateral MAPSE to clinical and imaging risk factors results in significant improvement in model fit (likelihood ratio test $P < .0001$) and C statistic (increasing from 0.675 to 0.844; $P < .0001$), with a continuous net reclassification improvement of 1.036 (95% CI: 0.878, 1.194).

Materials and Methods

Study Design

Four geographically diverse medical centers in the United States participated in this observational, multicenter study. The data coordinating center used a cloud-based database (CloudCMR, *www.cloudCMR.com*) containing de-identified searchable data from consecutive patients with full Digital Imaging and Communications in Medicine datasets from the participating centers (R.J.K. and R.M.J. have a proprietary interest in Heart IT, which owns and operates CloudCMR). Institutional review board approval was obtained at each center.

Implications for Patient Care

- Measurements of lateral MAPSE can be obtained from conventional cine cardiac MR images without the need for specialized pulse sequences, propriety software, or additional imaging time.
- Cardiac MR imaging is commonly used for the assessment of patients with reduced EF and heart failure; lateral MAPSE provides a simple additional prognostic marker for predicting death in this population, with few deaths in patients with relatively preserved lateral MAPSE (>9 mm) regardless of whether their EF was above or below 35%.
- These findings have potentially broad application because they were made in a large multicenter group of patients being evaluated for LV dysfunction regardless of underlying cause.

Study Population

Inclusion criteria were consecutive patients (n = 1060) with an EF of less than 50% who had undergone clinical cardiac MR imaging in 2011 for the assessment of LV dysfunction with both cine and late gadolinium enhancement (LGE) imaging at the four participating centers. Patients were excluded if lateral MAPSE assessment could not be performed owing to poor image quality (n = 9) and if they had previously undergone prosthetic mitral valve replacement (n = 11), leaving 1040 patients. These patients formed the study population. Baseline demographics were obtained by local site investigators at the time of the clinical study.

Cardiac MR Image Acquisition

Images were acquired by using phased-array receiver coils according to the routine imaging protocol at each site. A typical protocol included steady-state free-precession cine images acquired in multiple short-axis and three long-axis

https://doi.org/10.1148/radiol.2017170529

Content codes: CA MR

Radiology 2018; 286:452–460

Abbreviations:
CI = confidence interval
EF = ejection fraction
LGE = late gadolinium enhancement
LV = left ventricle
LVEF = LV EF
MAPSE = mitral annular plane systolic excursion

Author contributions:
Guarantors of integrity of entire study, S.R., A.F.F.; study concepts/study design or data acquisition or data analysis/interpretation, all authors; manuscript drafting or manuscript revision for important intellectual content, all authors; manuscript final version approval, all authors; agrees to ensure any questions related to the work are appropriately resolved, all authors; literature research, S.R., A.F.F.; clinical studies, S.R., A.F.F.; statistical analysis, S.R., A.F.F.; and manuscript editing, all authors.

Conflicts of interest are listed at the end of this article.

Figure 1

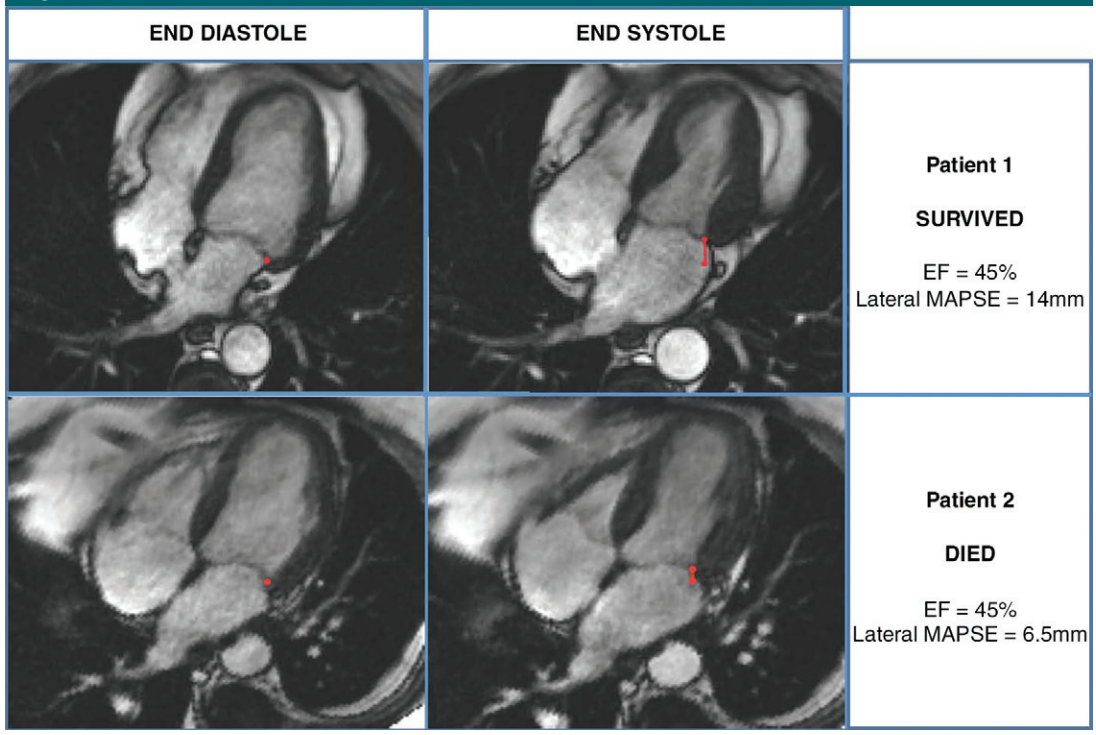

Figure 1: MR images demonstrate measurement of lateral MAPSE in a patient who survived (top) and a patient who subsequently died (bottom). Lateral mitral annular positions were recorded in four-chamber view at end diastole (images on left) and end systole (images on right), enabling measurement of lateral MAPSE (red line) in each patient.

views, with short-axis views obtained every 1 cm to cover the entire LV as previously described (6). LGE imaging was performed approximately 10–15 minutes after administration of a gadolinium contrast medium (0.15 mmol/kg) by using a two-dimensional segmented gradient-echo inversion-recovery sequence in the same views used for cine cardiac MR imaging.

Cardiac MR Image Analysis and MAPSE Assessment

The study site investigators (R.J.K., H.W.K., I.K., J.F.H., D.J.S., and A.F., all with more than 10 years of cardiac MR imaging experience) analyzed images on locally available workstations and were blinded to follow-up data. Delayed enhancement was determined by using the American Heart Association 17-segment model, as described previously (7–11).

Lateral MAPSE was measured as previously described (6). In brief, the lateral mitral annular position was marked at end diastole in the four-chamber view (Fig 1). Images were advanced frame by frame to the end of systole (just before opening of the mitral valve), where the lateral mitral annular position was again identified. Lateral MAPSE was defined as the distance between the lateral mitral annular position at the end of diastole to the lateral mitral annular position at the end of systole (Fig 1). Measurements were performed manually by one physician, who was blinded to patient outcomes and information (S.R., with 2 years of cardiac MR imaging experience). In 100 randomly selected patients, another cardiac MR imaging physician who was blinded to outcomes and information measured lateral MAPSE for the evaluation of interobserver variability (J.J., with 2 years of cardiac MR imaging experience). In another 100 randomly selected patients, the same physician (S.R.), who was still blinded to outcomes and information, obtained repeat measurements of lateral MAPSE approximately 5–6 months after the initial measurement to evaluate intraobserver variability.

Follow-up

Follow-up was completed in all patients for the primary outcome of all-cause mortality by using the United States Social Security Death Index. Time to event was calculated as the period between the cardiac MR study and death. Patients who did not experience the primary outcome were censored at the time of assessment.

Statistical Analysis

Normally distributed data were expressed as means ± standard deviations. Normality was assessed by using the Kolmogorov-Smirnov test. Intra- and interobserver variability was evaluated by using the Bland-Altman technique (12). Kaplan-Meier plots were used to evaluate the relationship between lateral

MAPSE and time to the primary outcome of all-cause mortality. We used Cox proportional hazards regression modeling to examine the independent association between lateral MAPSE and all-cause mortality and verified the proportionality assumption of all models. For the multivariable model, clinical and imaging risk factors that were univariate predictors (at $P \leq .15$) were considered as covariates. To evaluate the additional prognostic value of lateral MAPSE (as a continuous variable), the final model was compared with a model in which lateral MAPSE was not included. The log likelihoods of the two models were compared by using the likelihood ratio test. Model discrimination was compared by calculating the C statistic as well as the integrated discrimination improvement, which provides a measure of the improvement in sensitivity and specificity of the model with addition of the new predictor (lateral MAPSE) (13,14). Risk reclassification analyses were performed with calculation of continuous net reclassification improvement (13). $P < .05$ was considered indicative of a statistically significant difference. Analyses were performed by using STATA software (StataCorp, College Station, Tex).

Table 1

Baseline Characteristics Stratified according to Tertiles of Lateral MAPSE

Characteristics	All Patients ($n = 1040$)*	Lateral MAPSE <7.8 mm ($n = 346$)*	Lateral MAPSE 7.8–10.0 mm ($n = 345$)*	Lateral MAPSE >10.0 mm ($n = 349$)*	*P* Value
Mean age (y)†	59.5 ± 15.8	62.1 ± 16.2	60.1 ± 14.7	56.5 ± 16.0	<.001
Male (%)	676 (65.0)	227 (65.7)	209 (60.5)	238 (68.2)	.123
Mean BMI (kg/m^2)†	28.7 ± 8.5	28.7 ± 11.6	29.0 ± 6.5	28.5 ± 6.3	.700
Diabetes (%)	320 (30.8)	108 (31.2)	120 (34.9)	93 (26.8)	.071
Hyperlipidemia (%)	560 (53.9)	179 (51.7)	198 (57.5)	185 (52.9)	.282
Smoking (%)	149 (14.3)	48 (14.0)	44 (12.8)	56 (16.0)	.490
Hypertension (%)	695 (66.8)	239 (69.0)	248 (72.0)	210 (60.2)	.002
Aspirin (%)	653 (62.8)	219 (63.3)	242 (70.1)	194 (55.7)	.001
Statin (%)	575 (55.3)	181 (52.4)	206 (59.7)	188 (54.0)	.158
ACE inhibitor or ARB (%)	692 (66.6)	223 (64.4)	294 (70.7)	208 (59.7)	.077
Beta blocker (%)	513 (49.3)	181 (52.2)	133 (54.5)	146 (42.0)	.003
Diuretic (%)	466 (44.8)	186 (53.9)	163 (47.4)	119 (34.1)	<.001
LVEDV index (mL/m^2)†	117.4 ± 52.9	122.6 ± 60.6	119.4 ± 51.7	110.7 ± 45.0	.008
LVESV index (mL/m^2)†	66.3 ± 43.7	77.9 ± 53.1.8	68.0 ± 40.0	54.0 ± 32.9	<.001
LV mass index (g/m^2)†	113.8 ± 28.3	114.1 ± 41.0	110.2 ± 42.2	116.9 ± 45.1	.853
LGE present (%)	645 (62.0)	232 (67.2)	206 (59.7)	204 (58.4)	.043
LVEF (%)†	33.8 ± 10.0	29.4 ± 10.4	33.7 ± 9.4	38.0 ± 8.2	<.001

Note.—ACE = angiotensin converting enzyme, ARB = angiotensin receptor blocker, BMI = body mass index, LVEDV = LV end diastolic volume index, LVEF = LV EF, LVESV = LV end systolic volume index.

* Except where indicated, data are numbers of patients, with percentages in parentheses.

† Data are means ± standard deviations.

Results

Patient Characteristics

Table 1 summarizes baseline patient characteristics. All continuous variables were normally distributed. The mean age of the study population was 59.5 years ± 15.8. Of the 1040 patients, 676 (65%) were men. Three hundred twenty patients (30.8%) had diabetes mellitus. Two hundred ninety-one of the 1040 patients (28%) had a history of previous myocardial infarction, and 149 (14.3%) were smokers. Approximately 177 of the 1040 patients (17%) had LV hypertrophy (by using a cutoff of 95 g/m^2 for women and 115 g/m^2 in men). The mean EF was 33.8% ± 10.0; 645 of the 1040 patients (62%) had LGE present. About 48% of patients had an ischemic LGE pattern and 14% had a nonischemic pattern. Mean lateral MAPSE for the population was 9.1 mm. Median lateral MAPSE was 9.0 mm (interquartile range: 7.8–10.0 mm).

Inter- and Intraobserver Variability

Bland-Altman analysis of interobserver variability for lateral MAPSE showed a bias of 0.14 mm. The 95% limits of agreement were −2.18 to 1.90 mm (Fig 2). Bland-Altman analysis of intraobserver variability for lateral MAPSE showed a bias of −0.04 mm. The 95% limits of agreement were −1.57 to 1.64 mm (Fig 2).

Primary Outcome

Of the 1040 patients in the study, 132 died during a median follow-up of 4.4 years (interquartile range: 3.6–5.1 years).

Outcomes Stratified according to Lateral MAPSE

At Kaplan-Meier analysis, the risk of death increased significantly with decreasing tertiles of lateral MAPSE (log-rank $P = .0001$) (Fig 3). Kaplan-Meier analysis of patients with EF of 35% or less versus those with EF greater than 35% stratified by using lateral MAPSE above and below the median (9 mm) showed that mortality was significantly higher in patients with lower lateral MAPSE, irrespective of EF (Fig 4). Patients with LVEF of 35% or less and low lateral MAPSE had similarly reduced survival as those patients with LVEF greater than 35% and low lateral MAPSE (log-rank $P = .72$). Likewise, patients with LVEF of 35% or less and high lateral MAPSE had similar survival to those patients with LVEF greater than 35% and high lateral MAPSE (log-rank $P = .96$).

Kaplan-Meier analysis of patients with LGE versus those without LGE stratified according to the highest and lowest tertiles of lateral MAPSE showed that mortality was highest in the patients with both LGE and low lateral MAPSE (Fig 5). Patients with LGE and low lateral MAPSE had significantly reduced survival compared with those with LGE and high lateral MAPSE (log-rank $P < .0001$). Likewise, patients with low lateral MAPSE and no LGE had significantly reduced survival compared

Figure 2

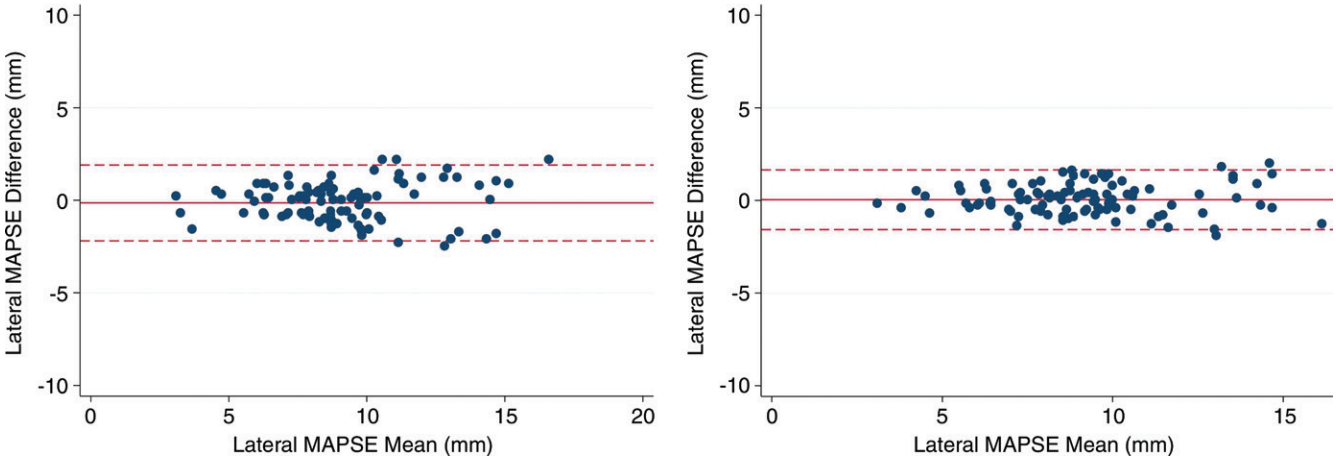

Figure 2: Bland-Altman analysis of lateral MAPSE for interobserver (left) and intraobserver (right) variability. Solid line represents bias, dashed lines represents 95% limits of agreement.

with those with high lateral MAPSE and no LGE (log-rank $P < .0001$).

Multivariable Analysis and Incremental Prognostic Value

After adjustment for clinical and imaging risk factors that were univariate predictors at $P \leq .15$ (age, body mass index, diabetes, LV end-diastolic volume index, LGE, EF), lateral MAPSE remained a significant independent predictor of death (hazard ratio = 2.051 per mm decrease; 95% confidence interval [CI]: 1.520, 2.768; $P < .001$) (Tables 2, 3). The addition of lateral MAPSE in this model resulted in a significantly improved model fit as assessed with the likelihood ratio test ($P < .0001$). In addition, there was an integrated discrimination improvement of 0.192 (95% CI: 0.133, 0.258) with a continuous net reclassification improvement of 1.036 (95% CI: 0.878, 1.194). Moreover, the addition of lateral MAPSE resulted in significant improvement in model discrimination as assessed with the C statistic (C statistic increased from 0.675 to 0.844; $P < .0001$).

These findings remain essentially unchanged when extent of LGE is used in our analysis instead of presence and/or absence of LGE. The extent of LGE is a univariable predictor of death in this population (hazard ratio = 1.029; 95% CI: 1.014, 1.044; $P < .0001$). Similarly, lateral MAPSE remains a significant predictor after adjustment for clinical and imaging predictors (hazard ratio = 2.147; 95% CI: 1.585, 2.907; $P < .0001$).

Figure 3

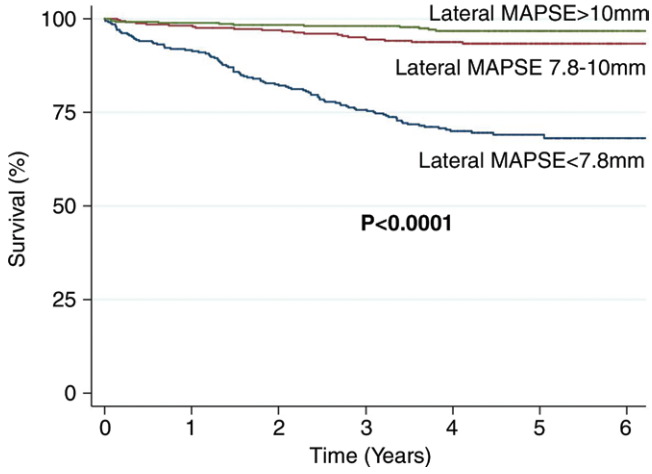

Figure 3: Kaplan-Meier curves for survival stratified according to tertiles of lateral MAPSE: lateral MAPSE less than 7.8 mm ($n = 346$), lateral MAPSE measuring 7.8–10 mm ($n = 345$), and lateral MAPSE greater than 10 mm ($n = 349$).

Discussion

This study shows that lateral MAPSE—as a surrogate for LV long-axis function—is a significant independent predictor of mortality in a large multicenter population of patients with LV dysfunction and reduced EF. Moreover, we demonstrated that this simple parameter provides prognostic information incremental to common clinical and imaging risk factors, including EF and LGE. A particular strength of these findings is that they were made in a large multicenter group of patients being evaluated for LV dysfunction regardless of the underlying cause. Thus, these findings have potentially broad application to this important patient group. Moreover, measurements of lateral MAPSE were obtained from standard cine cardiac MR images without

Figure 4

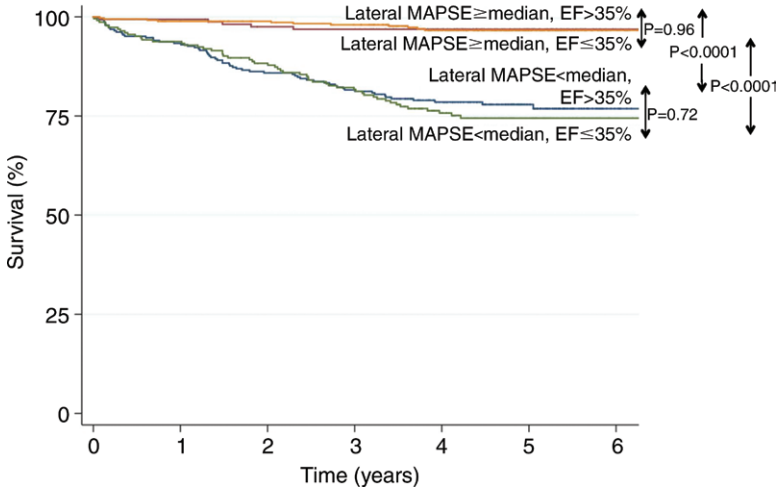

Figure 4: Kaplan-Meier curves of patients with EF of 35% or less versus those with EF greater than 35% stratified according to lateral MAPSE above and below the median (9 mm): lateral MAPSE less than 9 mm and EF of 35% or less ($n = 289$), lateral MAPSE less than 9 mm and EF greater than 35% ($n = 229$), lateral MAPSE of at least 9 mm and EF of 35% or less ($n = 161$), and lateral MAPSE of at least 9 mm and EF greater than 35% ($n = 361$).

Figure 5

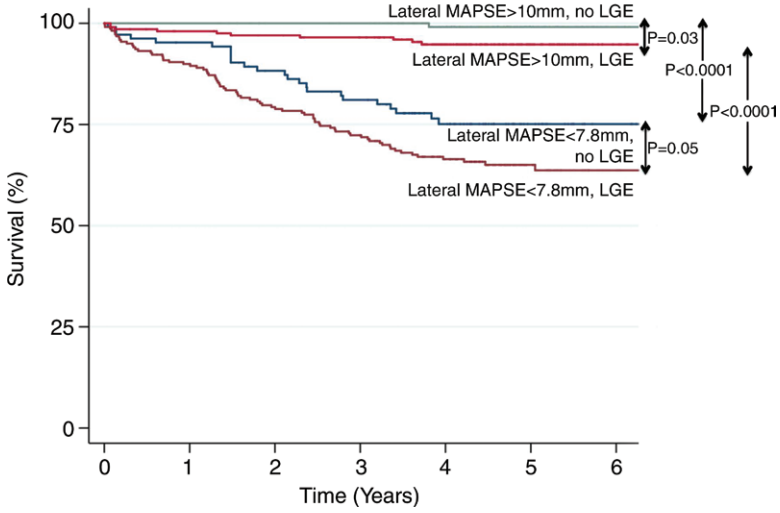

Figure 5: Kaplan-Meier curves of patients with LGE versus those without LGE stratified according to highest and lowest tertiles of lateral MAPSE: lateral MAPSE less than 7.8 mm and LGE ($n = 232$), lateral MAPSE less than 7.8 mm and no LGE ($n = 114$), lateral MAPSE greater than 10 mm and LGE ($n = 146$), and lateral MAPSE greater than 10 mm and no LGE ($n = 203$).

the need for propriety software or additional imaging time.

Long-Axis Function and MAPSE in Cardiac Mechanics

Long-axis function plays a fundamental role in cardiac mechanics, contributing to ventricular ejection by reducing long-axis LV cavity size as the mitral annulus is pulled toward the apex (2,15). Cardiac MR imaging has been used to measure the contribution of longitudinal mitral plane displacement to overall stroke volume in healthy subjects, elite athletes, and patients with dilated cardiomyopathy (1,2). These studies suggest that as much as 60% of stroke volume may be explained by longitudinal mitral annular motion. In diastole, the mitral annulus springs back to its equilibrium position moving around the column of blood passing through the mitral valve, thus aiding ventricular filling (15).

Possibly because of their subendocardial location, the more longitudinal myocardial fibers seem to be exquisitely sensitive to disturbance by various abnormalities; for example, mitral annular motion is very rapidly reduced by ischemia in experimental models (3,16).

Assessment of Long-Axis Function

Because the cardiac apex is fixed with respect to the chest wall, long-axis function can be assessed by measuring changes in the position of the mitral annulus (15). Initial studies used M-mode echocardiography to directly follow the position of the mitral annulus and measure MAPSE (17). Recently, echocardiographic two-dimensional speckle tracking techniques have evolved to assess long-axis function by measuring LV longitudinal strain (18). Strain imaging has the potential advantage of providing segmental and global information regarding longitudinal deformation rather than the monodimensional focal data derived from MAPSE. However, these echo strain techniques are highly dependent on attainment of good-quality images and there is lack of standardization among different vendors (5). Moreover, analysis can be time consuming and requires substantial operator experience (5,18). Recent developments in cardiac MR imaging feature tracking technology show promise in allowing measurement of longitudinal strain by using routine cine images in the clinical setting (19,20). In contrast to strain techniques, our simple measurement of lateral MAPSE can be performed easily without the need for proprietary software.

Cardiac MR Imaging Assessment of Long-Axis Function and Prognosis

There is a large and growing body of echocardiographic literature demonstrating the prognostic value of long-axis function by using both MAPSE and global

Table 2

Hazard Ratios for All-Cause Mortality of Lateral MAPSE Alone as Well as Adjusted in Clinical and Imaging Models

Model	Hazard Ratio	*P* Value
Lateral MAPSE	1.653 (1.521, 1.795)	<.001
Lateral MAPSE + clinical predictors	1.644 (1.511, 1.789)	<.001
Lateral MAPSE + imaging predictors	1.955 (1.470, 2.600)	<.001
Lateral MAPSE + clinical predictors + imaging predictors	2.051 (1.520, 2.768)	<.001

Note.—Hazard ratios are given per millimeter decrease. Numbers in parentheses are 95% CIs. Clinical predictors = age, body mass index, diabetes; imaging predictors = EF, LV end-diastolic volume index, LGE.

Table 3

Multivariable Model of Mortality with Lateral MAPSE Adjusted to Univariate Clinical and Imaging Predictors (at $P \leq .15$)

	Univariable Analysis		Multivariable Analysis	
Variable	Hazard Ratio	*P* Value	Hazard Ratio	*P* Value
Age	1.030 (1.017, 1.042)	<.001	1.019 (1.007,1.032)	.003
BMI	1.011 (1.000,1.022)	.109	1.012 (1.001,1.023)	.022
Diabetes	1.893 (1.338,2.677)	<.001	1.588 (1.110,2.272)	.011
LVEDV index	0.998 (0.994,1.001)	.148	1.000 (0.996,1.005)	.842
Lateral MAPSE*	1.653 (1.521,1.795)	<.001	2.051 (1.520,2.768)	<.001
LGE present	2.338 (1.540,3.551)	<.001	1.954 (1.276,2.992)	.002
LVEF†	1.018 (1.002,1.036)	.032	1.001 (0.948, 1.057)	.977

Note.—Numbers in parentheses are 95% CIs. BMI = body mass index, LVEDV = LV end diastolic volume.

* Per millimeter decrease.

† Per percentage decrease.

longitudinal strain in a wide variety of conditions including atrial fibrillation, after myocardial infarction, ischemic cardiomyopathy, heart failure (with reduced or preserved EF), aortic stenosis, tetralogy of Fallot, amyloidosis, after heart transplantation, and after anthracycline therapy (4,5).

Riffel et al (21) recently showed that mitral annular displacement with respect to the cardiac apex, measured with cardiac MR imaging, correlates well with echo-derived global longitudinal strain. However, studies specifically assessing the prognostic significance of LV long-axis function at cardiac MR imaging have been limited to date.

Rangarajan et al (6) recently showed that lateral MAPSE measured from four-chamber cine images is independently associated with adverse cardiovascular outcomes in 400 consecutive patients undergoing cardiac MR imaging. In contrast to our current study, their patient population included individuals with both reduced and preserved EF from a single center with relatively short follow-up and limited end points. Others have shown similar findings in patients with nonischemic cardiomyopathy, using a surrogate cardiac MR imaging measure of long-axis strain derived from the movement of the mitral annulus relative to the apex to predict a composite outcome of adverse cardiac events (22,23). Gjesdal et al (24) examined the prognostic value of similarly derived cardiac MR imaging long-axis function from 1651 individuals in the Multi-ethnic Study of Atherosclerosis cohort who were free of cardiovascular disease. After a median of 6.8 years of follow-up, long-axis function was found to be an independent predictor of cardiovascular outcomes (24). Using dedicated cardiac MR imaging feature-tracking software, Buss and colleagues (25) demonstrated that global longitudinal strain was an independent predictor of the composite end point of cardiac death, heart transplantation, and aborted sudden cardiac death in 210 patients with nonischemic dilated cardiomyopathy who were followed up for a median of 5.3 years.

The total number of hard events (n = 132) in our population is significantly higher than that in previous cardiac MR studies of long-axis function, which greatly increases the robustness of our observations.

Role of Cardiac MR Imaging in the Assessment of LV Dysfunction

Cardiac MR imaging has evolved into a major tool for the diagnosis and prognostic assessment of patients with LV dysfunction by providing data on morphologic characteristics, function, perfusion, viability, and tissue characterization (9,26–29). It is the standard of reference for measuring ventricular volumes, mass, and function, allowing serial assessment of disease progression or treatment response in individual patients (26–29). Cardiac MR imaging tissue characterization can help establish the underlying cause of a cardiomyopathy (26–29). LGE imaging allows assessment of the likelihood of recovery of function after revascularization, medical therapy, or cardiac resynchronization (26–29). LGE is a powerful predictor of adverse cardiovascular outcome in a wide range of cardiomyopathies (26–29). In this study, we have shown that lateral MAPSE provides independent prognostic information in patients with LV dysfunction undergoing cardiac MR imaging. Moreover, this was incremental to standard clinical and cardiac MR imaging variables, including LGE and EF. How this information will affect clinical care requires further study. However, it is interesting to note that we found that patients with relatively preserved lateral MAPSE (>9 mm) had very few deaths regardless of whether their EF was higher or lower than 35%. Given that current guidelines recommend implantable cardioverter defibrillator placement based primarily on an

EF of 35% or less, it will be interesting to specifically examine the role of lateral MAPSE for the prediction of sudden cardiac death in future studies.

Study Limitations

Baseline demographics were obtained by local site investigators at the time of the clinical study and were limited to the prespecified variables presented herein, which do not represent a comprehensive list of all possible prognostic markers. For example, plasma B-type natriuretic peptide levels were not routinely measured at the time of imaging and were not included in our predictive models. In addition, not all possible imaging variables were measured (eg, left atrial volume index).

Our findings were made in a large multicenter group of patients being evaluated for LV dysfunction regardless of underlying cause. We believe that this represents a major strength of this study because our observations have potentially broad application to this important patient group and greatly expand the evidence base for cardiac MR imaging–derived lateral MAPSE and prognosis.

Information regarding cause of death or specific cardiovascular outcomes such as myocardial infarction, sudden death, implantable cardioverter defibrillator placement, transplantation, revascularization, or hospitalization were not available. Follow-up data in this study were limited to the primary end point of all-cause death. However, many have argued that all-cause mortality is the most important and appropriate study end point because it is objective, clinically relevant, and unbiased, which is often not the case for cardiac death or softer outcomes such as revascularization or hospitalization (30–33).

Our simple lateral MAPSE measurements did not account for possible translational movements of the mitral annulus or for heart size differences, which may confound assessment of long-axis function. More complex methods for assessing mitral annulus long-axis motion include use of multiple long-axis views, with normalization to body size, or calculation of various changes in apex-to-annulus length expressed as a ratio of end-diastolic measurements (22,24). However, in this study we prospectively decided to measure the simplest possible parameter, lateral MAPSE, which has been shown to have prognostic significance in the echocardiography and cardiac MR imaging literature. We believe that simple rapid techniques are more likely to be used in busy clinical laboratories. Moreover, our results stand on their own and clearly demonstrate that this simple lateral MAPSE measurement is an important independent predictor of death, incremental to standard clinical and imaging variables.

In conclusion, in this large multicenter study, lateral MAPSE measured during routine cine cardiac MR imaging was a significant independent predictor of mortality in patients with LV systolic dysfunction–incremental to common clinical and imaging risk factors including EF and LGE. A major strength of these findings is that they were obtained in a large multicenter group of patients being evaluated for LV dysfunction regardless of underlying cause. Thus, these observations have potentially broad application to this important patient group. Future studies are warranted to explore the role of cardiac MR imaging–derived lateral MAPSE in clinical decision making for patients with LV dysfunction.

Disclosures of Conflicts of Interest: S.R. disclosed no relevant relationships. **R.M.J.** Activities related to the present article: disclosed no relevant relationships. Activities not related to the present article: disclosed no relevant relationships. Other relationships: has proprietary interest in HEART IT, which owns and operates CloudCMR; is an inventor on a U.S. patent on delayed-enhancement MR imaging owned by Northwestern University. **R.J.K.** Activities related to the present article: disclosed no relevant relationships. Activities not related to the present article: disclosed no relevant relationships. Other relationships: is co-founder of HeartIT; is an inventor on a U.S. patent on delayed-enhancement MR imaging owned by Northwestern University. **H.W.K.** disclosed no relevant relationships. **I.K.** disclosed no relevant relationships. **J.F.H.** disclosed no relevant relationships. **D.P.S.** disclosed no relevant relationships. **J.J.** disclosed no relevant relationships. **A.F.F.** disclosed no relevant relationships.

References

1. Carlsson M, Ugander M, Mosén H, Buhre T, Arheden H. Atrioventricular plane displacement is the major contributor to left ventricular pumping in healthy adults, athletes, and patients with dilated cardiomyopathy. Am J Physiol Heart Circ Physiol 2007;292(3):H1452–H1459.
2. Carlsson M, Ugander M, Heiberg E, Arheden H. The quantitative relationship between longitudinal and radial function in left, right, and total heart pumping in humans. Am J Physiol Heart Circ Physiol 2007;293(1):H636–H644.
3. Henein MY, Gibson DG. Long axis function in disease. Heart 1999;81(3):229–231.
4. Hu K, Liu D, Herrmann S, et al. Clinical implication of mitral annular plane systolic excursion for patients with cardiovascular disease. Eur Heart J Cardiovasc Imaging 2013;14(3):205–212.
5. Kalam K, Otahal P, Marwick TH. Prognostic implications of global LV dysfunction: a systematic review and meta-analysis of global longitudinal strain and ejection fraction. Heart 2014;100(21):1673–1680.
6. Rangarajan V, Chacko SJ, Romano S, et al. Left ventricular long axis function assessed during cine-cardiovascular magnetic resonance is an independent predictor of adverse cardiac events. J Cardiovasc Magn Reson 2016;18(1):35.
7. Kim RJ, Farzaneh-Far A. The diagnostic utility of cardiovascular magnetic resonance in patients with chest pain, elevated cardiac enzymes and non-obstructed coronary arteries. Rev Esp Cardiol 2009;62(9):966–971.
8. Kwong RY, Farzaneh-Far A. Measuring myocardial scar by CMR. JACC Cardiovasc Imaging 2011;4(2):157–160.
9. Abbasi SA, Ertel A, Shah RV, et al. Impact of cardiovascular magnetic resonance on management and clinical decision-making in heart failure patients. J Cardiovasc Magn Reson 2013;15:89.
10. Dandekar VK, Bauml MA, Ertel AW, Dickens C, Gonzalez RC, Farzaneh-Far A. Assessment of global myocardial perfusion reserve using cardiovascular magnetic resonance of coronary sinus flow at 3 Tesla. J Cardiovasc Magn Reson 2014;16:24.
11. McGraw S, Mirza O, Bauml MA, Rangarajan VS, Farzaneh-Far A. Downstream clinical consequences of stress cardiovascular magnetic resonance based on appropriate use criteria. J Cardiovasc Magn Reson 2015;17:35.
12. Bland JM, Altman DG. Statistical methods for assessing agreement between two methods of clinical measurement. Lancet 1986;1(8476):307–310.
13. Pencina MJ, D'Agostino RB Sr, D'Agostino RB Jr, Vasan RS. Evaluating the added predictive

ability of a new marker: from area under the ROC curve to reclassification and beyond. Stat Med 2008;27(2):157–172; discussion 207–212.

14. Pickering JW, Endre ZH. New metrics for assessing diagnostic potential of candidate biomarkers. Clin J Am Soc Nephrol 2012;7(8):1355–1364.
15. Henein MY, Gibson DG. Normal long axis function. Heart 1999;81(2):111–113.
16. Sanderson JE. Left and right ventricular long-axis function and prognosis. Heart 2008;94(3):262–263.
17. Zaky A, Grabhorn L, Feigenbaum H. Movement of the mitral ring: a study in ultrasoundcardiography. Cardiovasc Res 1967;1(2):121–131.
18. Shah AM, Solomon SD. Myocardial deformation imaging: current status and future directions. Circulation 2012;125(2):e244–e248.
19. Schuster A, Hor KN, Kowallick JT, Beerbaum P, Kutty S. Cardiovascular magnetic resonance myocardial feature tracking: concepts and clinical applications. Circ Cardiovasc Imaging 2016;9(4):e004077.
20. Pedrizzetti G, Claus P, Kilner PJ, Nagel E. Principles of cardiovascular magnetic resonance feature tracking and echocardiographic speckle tracking for informed clinical use. J Cardiovasc Magn Reson 2016;18(1):51.
21. Riffel JH, Andre F, Maertens M, et al. Fast assessment of long axis strain with standard cardiovascular magnetic resonance: a validation study of a novel parameter with reference values. J Cardiovasc Magn Reson 2015;17:69.
22. Riffel JH, Keller MG, Rost F, et al. Left ventricular long axis strain: a new prognosticator in non-ischemic dilated cardiomyopathy? J Cardiovasc Magn Reson 2016;18(1):36.
23. Arenja N, Riffel JH, Fritz T, et al. Diagnostic and prognostic value of long-axis strain and myocardial contraction fraction using standard cardiovascular MR imaging in patients with nonischemic dilated cardiomyopathies. Radiology 2017;283(3):681–691.
24. Gjesdal O, Yoneyama K, Mewton N, et al. Reduced long axis strain is associated with heart failure and cardiovascular events in the Multi-Ethnic Study of Atherosclerosis. J Magn Reson Imaging 2016;44(1):178–185.
25. Buss SJ, Breuninger K, Lehrke S, et al. Assessment of myocardial deformation with cardiac magnetic resonance strain imaging improves risk stratification in patients with dilated cardiomyopathy. Eur Heart J Cardiovasc Imaging 2015;16(3):307–315.
26. Karamitsos TD, Francis JM, Myerson S, Selvanayagam JB, Neubauer S. The role of cardiovascular magnetic resonance imaging in heart failure. J Am Coll Cardiol 2009;54(15):1407–1424.
27. Senthilkumar A, Majmudar MD, Shenoy C, Kim HW, Kim RJ. Identifying the etiology: a systematic approach using delayed-enhancement cardiovascular magnetic resonance. Heart Fail Clin 2009;5(3):349–367, vi.
28. Kim HW, Farzaneh-Far A, Kim RJ. Cardiovascular magnetic resonance in patients with myocardial infarction: current and emerging applications. J Am Coll Cardiol 2009;55(1):1–16.
29. Kramer CM. Role of cardiac MR imaging in cardiomyopathies. J Nucl Med 2015;56(Suppl 4):39S–45S.
30. Klem I, Shah DJ, White RD, et al. Prognostic value of routine cardiac magnetic resonance assessment of left ventricular ejection fraction and myocardial damage: an international, multicenter study. Circ Cardiovasc Imaging 2011;4(6):610–619.
31. Lauer MS, Blackstone EH, Young JB, Topol EJ. Cause of death in clinical research: time for a reassessment? J Am Coll Cardiol 1999;34(3):618–620.
32. Kim SG, Fogoros RN, Furman S, Connolly SJ, Kuck KH, Moss AJ. Standardized reporting of ICD patient outcome: the report of a North American Society of Pacing and Electrophysiology Policy Conference, February 9–10, 1993. Pacing Clin Electrophysiol 1993;16(7 Pt 1):1358–1362.
33. Stanton T, Leano R, Marwick TH. Prediction of all-cause mortality from global longitudinal speckle strain: comparison with ejection fraction and wall motion scoring. Circ Cardiovasc Imaging 2009;2(5):356–364.